Relation between Absorption and Emission in the Region of the R Lines of Ruby

D. F. NELSON AND M. D. STURGE
Bell Telephone Laboratories, Murray Hill, New Jersey
(Received 1 September 1964)

We have measured the radiative efficiency (ratio of R-line photons to the total number of photons emitted) and absorption cross sections for the R lines of dilute ruby, as a function of polarization and temperature between 20 and 373°K. We have also measured the fluorescent lifetime from 20 to 373°K in optically thin crystals, and from 20 to 273°K in optically thick crystals. The difference between the reciprocal lifetimes in thin and thick crystals is directly comparable (via the Einstein relations) with the integrated absorption in the R lines. This comparison shows that for the R lines at 20 and 77°K detailed balance holds to well within the experimental error of 5%, a precision never to our knowledge previously approached in solids. An upper limit of 0.002 cm^{-1} was placed on any Stokes shift of the R_1 line, confirming that it is a no-phonon line. Comparison of σ and α spectra confirms that the R lines and their vibronic satellites are predominately electric-dipole in character. The radiative efficiency of the R lines is strongly polarization dependent, a result which differs from that of previous workers. Its temperature dependence agrees well with that calculated from the observed vibronic spectrum at 77°K. The integrated absorption in the R lines increases by about 20% between 20 and 373°K. The absorption in the vibronic satellites on the high-frequency side of the R lines appears to be weaker than the corresponding emission on the low-frequency side. The temperature variation of the lifetime agrees well with that calculated from the absorption and radiative efficiency, but about 10% of the decay at 77°K and 30% at 373°K is either nonradiative or by emission at wavelengths outside the range of observation. The implications of our results for laser work are discussed.

1. INTRODUCTION

THE R_1 and R_2 lines of ruby (α-Al_2O_3:Cr^{3+}) are two closely spaced lines at the extreme red end of the visible spectrum which occur at the same wavelengths in absorption and emission. They arise from transitions between the ground state of the Cr^{3+} ion ($^4A_2$) and its first excited state (^2E).[1,2] (See Fig. 1.) Each of these cubic-field states is split by the combined action of the trigonal crystal field and spin-orbit coupling into a pair of Kramers doublets, 0.38 cm^{-1} apart in the ground state and 29.14 cm^{-1} apart in the ^2E state. The only other states in the vicinity of the ^2E states are the $^2T_1$ states,[3] 500 to 700 cm^{-1} above. The width of the R lines, about 12 cm^{-1} at room temperature, drops to less than 0.1 cm^{-1} at 20°K in good crystals, allowing the ground-state splitting to be clearly resolved below 100°K.

The R lines fluoresce with a quantum efficiency near unity[4] when the Cr^{3+} ion is excited, usually by pumping in its broad absorption bands in the green ($^4A_2 \rightarrow {}^4T_2$) and violet ($^4A_2 \rightarrow {}^4T_1$). The R lines are accompanied by nearby weak bands in both emission and absorption (not shown in Fig. 1) which extend over about 1000 cm^{-1} from the R lines and derive from the same electronic states of the Cr^{3+} ion. They arise from the creation or destruction of one or more quanta of lattice vibrational energy (phonons or local modes) simultaneously with the electronic transition. We refer to these bands as the vibronic satellites of the R lines. Although their peak intensity is very low, their integrated intensity is comparable with that of the narrow R lines. At sufficiently low temperatures phonons can only be emitted, not absorbed. Hence at such temperatures the satellites are entirely on the low-frequency side of the R lines in emission and on the high-frequency side in absorption. The ratio of the integrated emission

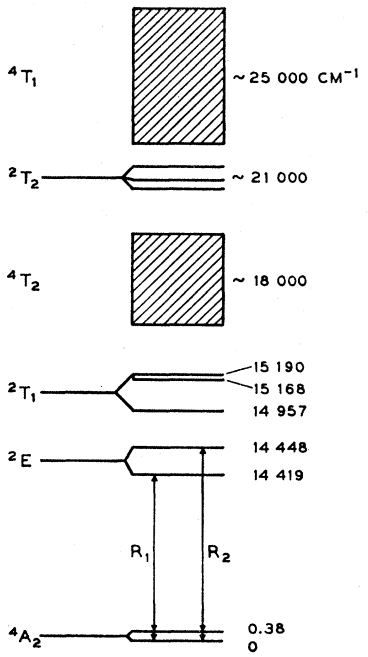

FIG. 1. Lower electronic energy levels of Cr^{3+} in Al_2O_3, designated by their representations in the O_h group. Transitions from the $^4A_2$ ground state to the broad bands $^4T_2$ and $^4T_1$ are spin allowed and relatively strong (oscillator strength $\sim 10^{-4}$), while those to the sharp levels ^2E, $^2T_1$, and $^2T_2$ are spin forbidden and have oscillator strengths $\sim 10^{-6}$.

[1] S. Sugano and Y. Tanabe, J. Phys. Soc. Japan **13**, 880 (1958).
[2] S. Sugano and I. Tsujikawa, J. Phys. Soc. Japan **13**, 899 (1958).
[3] J. Margerie, Compt. Rend. **255**, 1598 (1962).
[4] T. H. Maiman, R. H. Hoskins, I. J. d'Haenens, C. K. Asawa, and V. Evtuhov, Phys. Rev. **123**, 1151 (1961).

in the R lines to the total emission we call the radiative efficiency of the R lines.

The three quantities, radiative efficiency, integrated absorption cross section (or equivalently, the oscillator strength) and fluorescent lifetime, are closely related. Their magnitudes, and particularly their temperature dependence, are of great importance in the study of a fluorescent transition, both for the understanding of the fundamental processes occurring and for the use of the transition in a laser. In spite of the importance of the ruby laser and the consequent large amount of published work on the R lines, there are no really satisfactory data on these three quantities over a wide range of temperature in the literature. In particular, previous measurements of radiative efficiency have been vitiated by failure to recognize the importance of the polarization of the emitted light.[5,6] Furthermore, reported absorption data at low temperatures[2,7] are little more than order-of-magnitude estimates, partly because of the high resolution required and partly because of the difficulty of measuring Cr^{3+} concentration accurately. The latter gap has been filled by the careful work of Dodd *et al.*[8] While good lifetime data are available at high temperatures,[9,10] accurate measurements at low temperatures are hampered by self-absorption of fluorescence and so require more elaborate measurement techniques.

The R lines or ruby provide a system in which careful study of the relation between radiative efficiency, absorption and lifetime can be particularly rewarding. Large crystals of good quality are available; the fluorescence is strong and the quantum efficiency high; the R lines are genuine no-phonon lines with zero Stokes shift; the phonon wings, while strong enough to be measurable, are limited in extent; the R lines terminate on the ground state of the Cr^{3+} ion, their absorption being readily measurable with a high-resolution spectrometer; and a convenient and accurate method of measuring chromium concentration is available.[8] Furthermore, the detailed structure of the lower electronic energy levels of the Cr^{3+} ion in ruby (Fig. 1) is well understood in terms of conventional ligand field theory.[1,11,12] The principal difficulty in emission measurements at low temperatures is self-absorption of the R line radiation.[7] This can be overcome by use of small dilute crystals and sufficiently sensitive measuring apparatus, and can even be turned to good use since the lifetime in an optically thick crystal provides a direct measure of decay processes other than emission in the R lines. By means of lifetime and absorption measurements we have been able to check that detailed balance holds to within 5% for the R lines at low temperature, an accuracy vastly greater than that of previous measurements in solids (which have either been relative measurements[13] or, if absolute, accurate only in order of magnitude[7,14]) and as good or better than the accuracy obtained in atomic systems.[15–18]

2. RADIATIVE EFFICIENCY OF THE R LINES

The radiative efficiency of the R lines is defined as the ratio of the number of photons emitted in the R lines to the total number emitted by all mechanisms. In dilute ruby these mechanisms are the R lines, their associated vibronic transitions, and emission from the $^2T_1$ states, which is significant at temperatures above 250°K. The radiative efficiency should be distinguished from the quantum efficiency of the R lines which is defined as the number of photons emitted in the R lines divided by the number of photons absorbed by higher energy transitions. The radiative efficiency can be measured with considerably greater accuracy than the quantum efficiency since it is the ratio of two light intensities of nearby frequencies arising from the same (crystal) source while the quantum efficiency is a ratio of a fluorescent intensity from a crystal to a pumping intensity from a lamp in a different frequency band. The radiative efficiency is useful in interpreting the metastable ^2E state lifetime under conditions of strong self-absorption of the R lines and in predicting a radiative lifetime of the ^2E state in dilute ruby from absorption measurements in the R lines alone, subjects which will be discussed in later sections of the paper.

The radiative efficiencies of the R lines in dilute ruby in the two polarizations ($\eta_{\parallel}$ for $E\|c$ and $\eta_{\perp}$ for $E\perp c$) have been measured at temperatures characteristic of boiling hydrogen, boiling nitrogen, dry ice (in methyl alcohol), freezing water, and boiling water. A grating-equipped Perkin-Elmer Model 112 spectrometer was used to scan the spectrum between 6200 and 7800 Å. Some measurements were also made with a Jarrell-Ash 1.8-m grating spectrometer. A cooled RCA 7102 photomultiplier was used as a detector in all measurements de-

[5] G. Burns and M. I. Nathan, J. Appl. Phys. **34**, 703 (1963).
[6] N. A. Tolstoi and A. P. Abramov, Opt. i Spektroskopiya **14**, 691 (1963) [English transl.—Opt. Spectry. (USSR) **14**, 365 (1963)].
[7] F. Varsanyi, D. L. Wood, and A. L. Schawlow, Phys. Rev. Letters **3**, 544 (1959).
[8] D. M. Dodd, D. L. Wood, and R. L. Barns, J. Appl. Phys. **35**, 1183 (1964).
[9] C. Billington, Phys. Rev. **120**, 710 (1960).
[10] N. A. Tolstoi and Liu'Shun-Fu, Opt. i Spektroskopiya **13**, 403 (1962) [English transl.—Opt. Spectry. (USSR) **13**, 224 (1962)].
[11] S. Sugano and M. Peter, Phys. Rev. **122**, 381 (1961).
[12] R. M. Macfarlane, J. Chem. Phys. **39**, 3118 (1963).
[13] J. R. Haynes, M. Lax, and W. F. Flood, in *Proceedings of the International Conference on the Physics of Semiconductors, Prague 1960* (Czechoslovakian Academy of Sciences, Prague, 1961), p. 423.
[14] G. K. Wertheim, Phys. Rev. **104**, 662 (1956); A. R. Beattie and P. T. Landsberg, Proc. Roy. Soc. (London) **A258**, 486 (1960).
[15] W. Kuhn, Naturwiss. **14**, 48 (1926); M. W. Zemansky, Z. Physik **72**, 587 (1931).
[16] R. Ladenberg and E. Thiele, Z. Physik **72**, 697 (1931); H. H. Hupfield, Z. Physik **54**, 484 (1929).
[17] W. Zehden and M. W. Zemansky, Z. Physik **72**, 442 (1931); P. H. Garrett, Phys. Rev. **40**, 779 (1932).
[18] See A. C. G. Mitchell and M. W. Zemansky, *Resonance Radiation and Excited Atoms* (Cambridge University Press, Cambridge, England, 1934) for further references.

scribed in this paper. The relative signal obtained with this system per incident photon was determined as a function of wavelength for each polarization using a calibrated tungsten lamp of known temperature as the input and the recorded fluorescent signal corrected accordingly. An Osram HBO-200 lamp excited the ruby through 5 cm of saturated $CuSO_4$ solution. The ruby crystal used for measurements at 195, 273, and 373°K was 0.50 cm thick in the direction of measurement and had a chromium concentration of 1.8×10^{18} cm^{-3}. The crystal used at 20 and 77°K was 0.048 cm thick in the direction of measurement and had 1.1×10^{18} Cr^{3+} ions cm^{-3}. Self-absorption of the R lines is negligible for such samples at the temperatures used. The polarizing element used was type HN38 Polaroid. The sample was oriented with respect to the c axis to about 2°. The polarizer was oriented more accurately than this by rotating the polarizer and tipping the crystal to minimize the signal from the R_1 line for $E\|c$. Lineage in the crystals prevents perfect alignment. In order to check the alignment, the ratio of intensities of the R_1 line to the R_2 line in π polarization ($E\|c$) was compared with the measured absorption strengths modified by the expected population ratio at the temperature being studied. These procedures are very important because of the large dichroism of the R lines. In spite of these precautions, substantial corrections for imperfect polarization had to be made to the $E\|c$ spectrum at 20°K, and the value of $\eta_{\|}$ at this temperature is consequently somewhat inaccurate.

The results are shown in Fig. 2. The radiative efficiency is seen to rise at low temperatures to 0.83 for the σ polarization ($E\perp c$), which is stronger in emission, and to 0.49 for the π polarization ($E\|c$), which is weaker in emission. A discussion of the calculated curves shown in Fig. 2 will be given in Sec. 7.

The fact that the observed $\eta_{\perp}$ is independent of temperature below 77° to within the relative accuracy of ±0.01 shows that it is the same, to within ±0.03, for both the R lines. If it were not the same, the change with temperature of the relative population of the initial states would be reflected in a change in the measured radiative efficiency. Such a change is indeed observed for $\eta_{\|}$, which is substantially lower at 20° than at 77°. Because of the low accuracy of the 20° measurement, we can only say that for the R_2 line $\eta_{\|}$ must be greater than 0.60, while for the R_1 line, $\eta_{\|}=0.37\pm0.07$. These estimates are made on the assumption that the true $\eta_{\|}$ for each line separately is independent of temperature below 77°, but the qualitative conclusion that $\eta_{\|}$ is different for the two lines is independent of this assumption.

Burns and Nathan[5] have also measured the radiative efficiency of ruby as a function of temperature. Their results, which are for an undetermined polarization, differ substantially from ours. Judging by the size and concentration of their crystal, self-absorption of the R lines was probably important at the lower temperatures.[19] Tolstoi and Abramov[6] avoided this source of error by using thin polycrystalline layers, but these authors disclaim any intention of making quantitative intensity measurements.

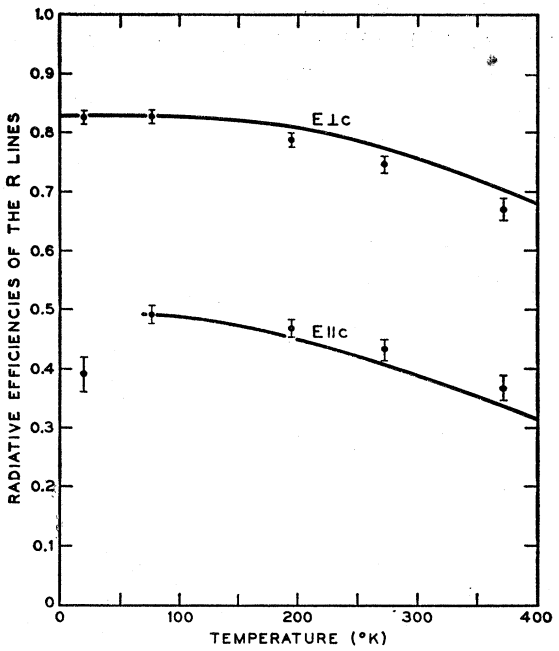

FIG. 2. Radiative efficiency of the R lines of ruby for $E\perp c$ and $E\|c$ as a function of temperature—Eq. (20).

For the measurements of the radiative efficiency the $\sigma(E\perp c, B\|c)$ and $\pi(E\|c, B\perp c)$ spectra have been used. The $\alpha(E\perp c, B\perp c)$ spectrum has also been observed at 77°K and found to be the same as the σ spectrum. This shows that both the R lines and the associated vibronic transitions are predominantly electric dipole in character. The former of these two conclusions has previously been shown to follow from the dichroism and the Zeeman effect.[1,2]

3. ABSORPTION MEASUREMENTS

The absorption in the R lines was measured in σ and π polarization at 20°, 77°, 195°, 273°, and 373°K. The α spectrum was checked at 77°. At 195°K and below, the ruby crystal was placed in the exit optics of a Jarrell-Ash 1.8-m spectrometer with a spectral slit width of 0.06 cm^{-1}. At 273 and 373°K, a Cary Model 14 spectrophotometer was used, with a spectral slit width of about 5 cm^{-1}. An empirical correction was made for the effect of the finite slit of the Cary spectrophotometer on the measured integrated absorption.

The crystals used were cut from Linde disc boules and each of the two components of the R_1 line which arise from the ground-state splitting had a linewidth of about

[19] We are grateful to Dr. Burns and Dr. Nathan for lending us the ruby crystal used in their experiment, and thus enabling us to check this assertion.

0.1 cm^{-1} at 20°K. Two concentations of chromium were used, 1.70×10^{18} and 2.31×10^{19} cm^{-3}. These concentrations are low enough for the number of Cr-Cr pairs to be negligible relative to the number of isolated ions.[20] The integrated absorption cross sections of specimens of the two concentrations at the same temperature agreed to within 3%. The concentrations were measured by optical absorption[8] (calibrated by x-ray fluorescence) and checked by neutron activation on four samples cut from a crystal of each concentration. The two methods agreed to within $2\frac{1}{2}$%, and the concentrations are believed to be accurate to within 3%. The Cr^{3+}, as opposed to the Cr, concentration, was checked by spin resonance on one specimen, containing 1.7×10^{18} Cr atoms cm^{-3}, to be $(1.9\pm0.3)\times10^{18}$ Cr^{3+} cm^{-3} (unfortunately the spin density in the reference specimen, phosphorus-doped silicon, was only known to ±15%). No evidence was found for spin resonance due to any other valence state of chromium. Since Cr^{6+} is nonmagnetic, inclusions of CrO_3, such as have been found in microscopic quantities in some crystals,[21] could not have been detected by this method. Perhaps stronger, though less direct, evidence that substantially all the chromium is in the trivalent state is supplied by the strict proportionality of the absorption in the broad bands to chromium concentration.[8] It is unlikely that the ratio of Cr^{3+} to chromium concentration, if different from unity, would be constant while the chromium concentration itself is varied by a factor of 300.

As predicted theoretically[22] the line shape at temperatures where thermal broadening is dominant is Lorentzian. This is illustrated in Fig. 3, which shows the absorption measurement on the R_1 line at 195°K, compared with Lorentzian and Gaussian profiles. The ground-state splitting of 0.38 cm^{-1} and Gaussian strain broadening of 0.1 cm^{-1} have been taken into account in calculating the curves. The experimental points fit the Lorentzian curve well over the range of measurement, but the experimental sensitivity is not sufficient to include all of the long tails characteristic of a Lorentzian profile, which are lost in the noise. If we measure the area under a smooth curve drawn through the experimental points, we exclude these tails, and are effectively cutting off the Lorentzian at a certain distance ν_c from the center of the line. The fraction of the total area thus excluded, assuming that the tails continue to be Lorentzian, is

$$\frac{2}{\pi\gamma}\int_{\nu_c}^{\infty}\frac{d\nu}{1+(\nu/\gamma)^2}=\frac{2}{\pi}\cot^{-1}(\nu_c/\gamma), \qquad (1)$$

where 2γ is the width of the line. For $\nu_c\gg\gamma$, the excluded fraction is $2\gamma/\pi\nu_c$. In the present case $\nu_c=10$ cm^{-1}, $\gamma=1.45$ cm^{-1} so the excluded area is 9% of the total and cannot be neglected. Neglect of the tails also gives a slight error in the baseline. The correction for this is usually small, about 2 or 3%.

At 77°K the situation is more complicated because the observed profile is the convolution of a Gaussian profile due to strain and instrumental broadening (which approximates to a Gaussian) with a Lorentzian due to thermal broadening of comparable magnitude. Furthermore, the lines due to the four different isotopes of Cr, while not resolved as they are at 20°K, are sufficiently separated to affect the line shape appreciably.[23] The convolution of a Gaussian and Lorentzian is called a Voigt profile and has been calculated by Posener and

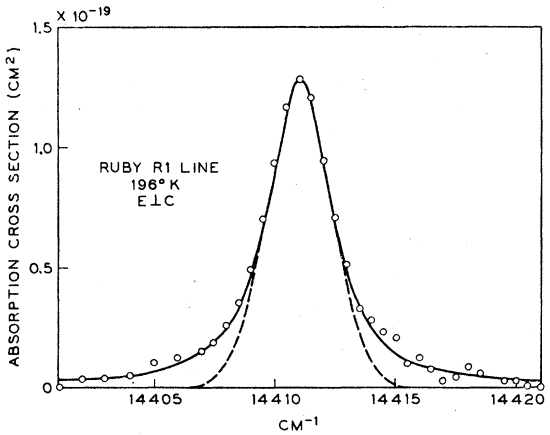

FIG. 3. Absorption in the R_1 line at 195°K ($E\perp c$); —Lorentzian profile; – – – Gaussian profile.

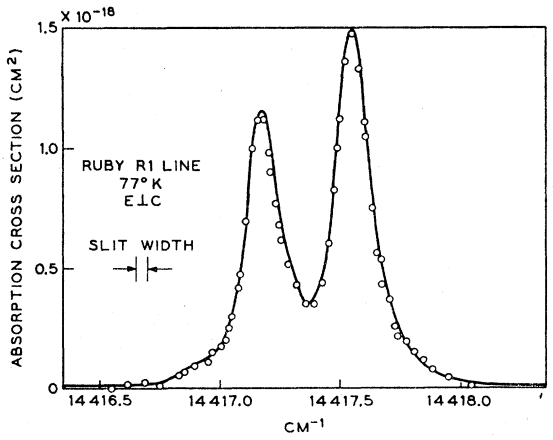

FIG. 4. Absorption in the R_1 line at 77°K ($E\perp c$). Sum of eight Voigt profiles calculated as described in the text.

[20] A. L. Schawlow, D. L. Wood, and A. M. Clogston, Phys. Rev. Letters **3**, 271 (1959).

[21] G. Eckhardt and A. L. Gentile, Bull. Am. Phys. Soc. **9**, 66 (1964).

[22] D. E. McCumber and M. D. Sturge, J. Appl. Phys. **34**, 1682 (1963); D. E. McCumber, Phys. Rev. **133**, A163 (1964); D. E. McCumber, J. Math. Phys. **5**, 221 (1964).

[23] A. L. Schawlow in *Advances in Quantum Electronics*, edited by J. R. Singer (Columbia University Press, New York, 1961), p. 50; G. F. Imbusch, W. M. Yen, A. L. Schawlow, G. E. Devlin, and J. P. Remeika, Phys. Rev. **136**, A481 (1964).

TABLE I. Absorption data for the R lines at 77°K. The peak absorption cross sections are the observed peak absorption coefficients divided by the number of ions in the initial state (i.e., by half the chromium concentration). The "observed" integrated absorption cross sections contain the various corrections described in Sec. 3.

Line	Initial substate of $^4A_2M_s$	Final substate of ^2E	$\sigma_\perp$ (peak) 10^{-18} cm^2	$\int\sigma_\perp d\nu$ (obs.) 10^{-19} cm	$\int\sigma_\perp d\nu$ (theor.) 10^{-19} cm	$\sigma_\parallel$ (peak) 10^{-18} cm^2	$\int\sigma_\parallel d\nu$ (obs.) 10^{-19} cm	$\int\sigma_\parallel d\nu$ (theor.) 10^{-19} cm
R_{1a}	$\pm\frac{1}{2}$	$\bar{E}$	1.2	2.4	2.4	0.14	0.35	0.9
R_{1b}	$\pm\frac{3}{2}$	$\bar{E}$	1.5	3.4	3.6	0.02	0.04	0
R_{2a}	$\pm\frac{1}{2}$	$2\bar{A}$	1.4	3.4	3.6	0.02	0.03	0
R_{2b}	$\pm\frac{3}{2}$	$2\bar{A}$	0.05	0.1	0	0.28	0.66	2.7

Van der Hulst and Reesinck.[24] For present purposes we assume the Gaussian contribution to the linewidth (due to strain and instrumental broadening) to be the same at 77°K as it is at 20°K, where thermal broadening is negligible and the profile is purely Gaussian. Taking the observed linewidths at 20°K (0.12 cm^{-1}) and at 77°K (0.15 cm^{-1}) we used Posener's tables[24] to find the Lorentzian contribution 2γ at 77°K to be 0.065 cm^{-1}. The sum over isotopes of Voigt profiles with these characteristics for the two components of the R_1 line is shown in Fig. 4 and compared with the experimental points. The agreement is excellent, but as before the tails, which are still essentially Lorentzian, are too weak to be observed. The area under the tails is still given by Eq. (1), with 2γ now 0.065 rather than the observed linewidth. This correction is between 2 and 5%.

A small but systematic error is introduced by imperfect polarization, the finite aperture of the beam, and by misalignment of the specimen. When studying absorption of σ-polarized light ($E\perp c$), π-polarized light ($E\|c$) is only weakly absorbed, and thus the peak absorbance is underestimated. In π polarization the absorbance is correspondingly overestimated. These errors can be substantial in a crystal grown by flame fusion because lineage can produce misorientation of the bulk crystal of up to 3° relative to the surface layers which are probed by x rays.[25] Careful choice of optical path, through a selected crystal, reduced this error to about 1°. We estimate the integrated absorption cross section to be $(2\pm2\%)$ low for $E\perp c$ and to be $(5\pm5)\times10^{-20}$ cm^2 high for $E\|c$ because of imperfect polarization. These corrections have been made to the integrated absorption but not to the peak values, which represent the raw experimental data.

In Table I, the results at 77°K are presented in terms of the absorption cross section σ. For a given transition, this is defined as α/N, where N is the concentration of ions in the initial state in cm^{-3} and α is the observed absorption coefficient in cm^{-1}. In the case of a g-fold degenerate initial state, $N=N_0/g$ for each substate, where N_0 is the total number of ions, so $\alpha=N_0\sum_i\sigma_i/g$, where the σ_i are the cross sections for transitions from the individual substates. Thus the "observed" cross section, α/N_0, is the *mean*, not the sum, of the σ_i. This is important when comparing the integrated absorption of an R line at high temperatures, where the ground-state doublet is not resolved, with that at low temperatures where it is.

The "theoretical" intensities in Table I are calculated from the observed absorption in the $^4A_2\rightarrow{}^4T_2$ (green) band[26] (from which the R lines derive their intensity through the spin-orbit coupling) using the formulas of Sugano and Tanabe[1] and the parameters of Sugano and Peter ("Calc. I").[11] The parameters of Macfarlane[12] give essentially the same results. The ratios of the different components, however, are independent of parameters and the deviation from the theoretical ratio in π polarization is probably connected with the vibronic problem. The calculated intensities have not been corrected for any "borrowing" of intensity by the vibronic satellites, as we do not know (see below) how much borrowing occurs. The absorption in σ polarization is in fortuitously good agreement with that predicted, considering the many uncertainties in the calculation. The measured π absorption, on the other hand, is substantially less than predicted. This is probably due to the fact that the strength of the $^4T_2$ band in π polarization is for the most part vibronically induced,[26] and cannot contribute to the strength of the (no-phonon) R lines (it does, of course, contribute to the vibronic satellites). In fact, the very observation of the R lines in π polarization is in itself evidence that some of the intensity (about $\frac{1}{4}$) of the $^4A_2\rightarrow{}^4T_2$ band in this polarization is *not* vibronically induced but would still be there in the absence of vibronic interactions.[27]

The coincidence of the σ and α spectra of the R lines shows that magnetic-dipole transitions are not important; we expect them to be about as strong[28] as in MgO:Cr^{3+} or about 1/30 the strength of the electric-dipole transitions observed in ruby. They may con-

[24] D. W. Posener, Australian J. Phys. **12**, 184 (1959); H. C. Van der Hulst and J. J. M. Reesinck, Astrophys. J. **106**, 121 (1947).

[25] R. L. Barns, in *Metallurgy of Advanced Electronic Materials*, edited by G. E. Brock (Gordon Breach, Science Publishers, Inc., New York, 1963), p. 337.

[26] D. S. McClure, J. Chem. Phys. **36**, 2757 (1962).

[27] Other explanations are possible; for instance the R lines could be deriving their intensity in π polarization directly from doublet states in the charge transfer band through the odd-parity crystal field; it would however be a surprising coincidence if such a derivation gave the same, approximately correct, ratios of the components as does the derivation from the $^4T_2$ band.

[28] S. Sugano, A. L. Schawlow, and F. Varsanyi, Phys. Rev. **120**, 2045 (1960).

TABLE II. Integrated absorption in the R lines (averaged over the two components of the ground state) as a function of temperature. The sixth column gives the reciprocal lifetime calculated from Eq. (9), the seventh column the reciprocal of the observed lifetime, and the last column, the discrepancy between them (see Sec. 6).

T °K	$\int_{R_1}\sigma_\perp d\nu$ 10^{-19} cm	$\int_{R_1}\sigma_\parallel d\nu$ 10^{-19} cm	$\int_{R_2}\sigma_\perp d\nu$ 10^{-19} cm	$\int_{R_2}\sigma_\parallel d\nu$ 10^{-19} cm	Calc. τ^{-1} sec^{-1}	Obs. τ^{-1} sec^{-1}	$(\tau^{-1})_{\text{obs.}} - (\tau^{-1})_{\text{calc}}$ sec^{-1}
20	2.9	0.2	1.7_5	0.3_5	235±12	262±3	27±12
77	2.9_3	0.2	1.7_5	0.3_5	213±9	239±3	26±9
195	2.9	0.1_7	1.8_5	0.4_2	215±11	249±5	34±12
273	3.3	0.2_3	1.8	0.4_3	237±15	280±3	43±16
300	3.5_5	0.2_2	1.9	0.4_4	244±15	294[a]	50
373	3.7_5	0.2_5	2.0	0.5	277±14	410±4	133±16

[a] Reference 10.

tribute slightly to the π absorption, but the intensities observed in the "wrong" polarization noted in Table I more probably represent experimental error due to imperfect polarization.

The integrated absorption in the R_1 and R_2 lines is given as a function of temperature in Table II. The figures for 20 and 77°K are averaged over the two components of each line, so as to be directly comparable with the measurements at higher temperatures, where the ground-state splitting is not resolved. At 373°K the exact distribution of integrated absorption between R_1 and R_2 is uncertain because of overlap of the lines.

The most interesting feature of Table II is the increase in strength of the R lines with temperature. If the electric-dipole matrix element for the electronic transition were independent of temperature, the R-line intensity would go down as that of the satellites goes up. The fact that the R lines increase with temperature is therefore evidence that the matrix element does too. This matrix element is proportional to the odd-parity component of the crystal field at the Cr^{3+} ion, which mixes odd-parity states of high energy into the even-parity d states between which we observe transitions. This odd-parity field has a static component arising from the fact that the Cr^{3+} ion is not at a center of symmetry in the crystal, and a dynamic component due to the existence of odd-parity lattice vibrations. At low temperatures, the strength of the no-phonon line is entirely due to the static component. The vibronic satellites not only derive strength from the static component via even-parity lattice vibrations, but also can have additional strength arising from odd-parity vibrations. A general phonon does not have a definite parity, even in a system with a center of symmetry, and can contribute to both effects. Both the static and dynamic odd-parity crystal fields can change with temperature. The increase in the dynamic field with temperature, due to the increasing number of phonons, affects primarily the vibronic satellites; it can, however, also increase the strength of the no-phonon line by simultaneous emission and absorption of a phonon. The relative weakness of two phonon processes in the vibronic satellites suggests that this will be a small effect.

The static component of the crystal field is extremely sensitive to the exact position of the Cr^{3+} ion in the lattice.[26,29] The mean position of the ion can change with temperature owing to thermal expansion (movement parallel to the c axis is permitted by the D_{3d}^6 space group of α-Al_2O_3) and the crystal field can increase or decrease as a consequence.

Even without a change in mean position of the ion, the greater amplitude of vibration at higher temperatures can cause the ion to sample a different crystal field, and the mean static crystal field will in general increase with temperature.

The possibility of a Stokes shift (difference between the frequencies of emission and absorption) of the R_1 line was explored with a crystal in the entrance optics of the Jarrell-Ash spectrometer, fluorescence and absorption spectra being obtained in quick succession by switching filters. Any Stokes shift at 4°K is less than 0.002 cm^{-1}. This result has been confirmed independently at temperatures up to 153°K by Brault *et al.*[30] The absence of a Stokes shift confirms that the R lines are genuine no-phonon lines.[23]

The vibronic satellites of the R lines, which are readily observable in emission, are very difficult to see in absorption because of their extremely small intensity. A heavily concentrated crystal cannot be used because absorption due to pairs of chromium ions partially obscures the wanted absorption due to the unpaired ions. On the other hand, measurements of the absorption in a 19-cm-thick crystal of ruby (Cr^{3+} concentration: 1.8×10^{19} cm^{-3}) failed to give quantitative results owing to the experimental difficulty of establishing a zero-absorption level. For these reasons we turned to the excitation spectrum, as a means of measuring the weak absorption. The intensity of fluorescence in the region of 14 000 cm^{-1} was observed as a function of exciting frequency, from 14 400 to 15 300 cm^{-1}. Except in the R lines themselves, the absorption is always weak, and so

[29] J. O. Artman and J. C. Murphy, J. Chem. Phys. 38, 1544 (1963).

[30] J. W. Brault, P. J. Warter, Jr., and R. U. Martinelli, Bull. Am. Phys. Soc. 9, 281 (1964). Note that O. Deutschbein [Ann. Physik 14, 729 (1932)] found a Stokes shift of 0.4 cm^{-1} for R_1 and 0.3 cm^{-1} for R_2. However, this was in ruby of relatively high concentration (about 1%) in which the R lines were about 4 cm^{-1} wide at 77°K.

the intensity of fluorescence is directly proportional to the absorption coefficient at the exciting frequency. At two points, 14 960 and 15 175 cm^{-1}, the absorption is strong enough to measure in a 5-cm-thick crystal. By comparing at these points we can convert to absolute absorption. Measurements were made at 77° with both polarizations of exciting light. The $E\|c$ spectrum is not very accurate owing to the large angular aperture of exciting light, which was necessary to get a large enough signal. The result for $E\perp c$ is shown in Fig. 5. To the right of 14 400 cm^{-1} is the excitation spectrum, normalized to absolute absorption at 14 960 and 15 175 cm^{-1}. To the left is the emission spectrum, normalized to give the same integrated area under the R lines as in absorption. The spectral slit width is 7–10 cm^{-1} for both spectra. The strong peaks at 14 960 and 15 175 cm^{-1} (the latter a partly resolved doublet) have been identified unambiguously by Margerie[3] as being due to the $^4A_2 \rightarrow {}^2T_1$ transitions. The great width of the no-phonon lines originating from the $^2T_1$ levels is presumably due to the fact that single phonon transitions to the ^2E levels are possible, with consequent lifetime broadening. The $^2T_1$ lines have their own relatively weak vibrational satellites in the region 15 200–16 000 cm^{-1}. The true vibrational satellites of the R lines are visible in absorption between the $^2T_1$ and the R lines, and (possibly) between the $^2T_1$ lines. Particular features of the emission spectrum,[31] such as the sharp peak 375 cm^{-1} from the R_1 line, are observable in the corresponding positions of the absorption spectrum. They are, however, weaker by 30% or more in the absorption spectrum and it is reasonable to suppose that this is true for the whole vibronic spectrum in absorption.

The R lines are transitions very weakly coupled to the lattice, and one would expect the vibronic states associated with the ^2E state (which are observed in absorption) to be substantially the same as those associated with the $^4A_2$ ground state. In this case the absorption and emission spectra should be mirrored in the R line (apart from small corrections due to the R-line splitting). Such mirror symmetry is observed, for instance, in the "red center" of ZnTe.[32] Additional evidence for the lack of symmetry between phonon-assisted absorption and emission is found in the emission at high temperatures (see Fig. 7); this is discussed in Sec. 7.

Two qualitative explanations for the lack of mirror symmetry come to mind. One is interaction with the $^2T_1$ levels, which might make the distribution of vibronic states different in the excited electronic state from that in the ground state. Such a difference might arise, for example, from the degeneracy of a state of

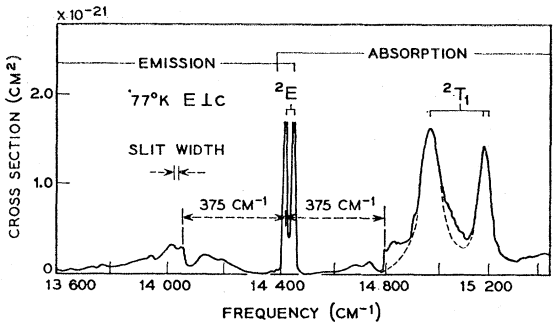

FIG. 5. Emission and "absorption" (actually excitation) spectra of dilute ruby in the region of the R lines at 77°K ($E\perp c$). The emission spectrum is normalized to give the correct area of the R lines and has been converted to a cross section by the formula $\sigma(\omega)=\lambda^2 A(\omega)=\mu_r\lambda^4 A(\lambda)$; the excitation spectrum is normalized to give the correct absorption at the peak of the $^2T_1$ lines. The concentration of ruby used for the excitation spectrum was 2.4×10^{19} cm^{-3}, sufficiently high for lines due to Cr-Cr pairs to be visible in the excitation spectrum. These lines were identified by comparison with the spectrum of a concentrated ruby (2×10^{20} cm^{-3}) and have been subtracted from the curve shown.

type (^2E+vibration) with a purely electronic $^2T_1$ state. However, one's qualitative impression from Fig. 5 is that the shape of the satellites is the same in absorption as in emission; apparently only their strength is different. An explanation in terms of changes in vibronic density of states therefore seems unlikely. The second possibility is that while the density of vibronic states is independent of the electronic state of the ion, the matrix element for vibronic transitions is not. It would have to be smaller when the ion is in the excited electronic state. If, as is probable, these transitions are vibronically induced, the matrix element depends on the odd-parity component (referred to the Cr^{3+} ion as origin) of the vibration involved. We expect the size of this component to be as sensitive as the crystal field to the position of the ion in the lattice. As remarked above, the position of the Cr^{3+} ion on the c axis is not determined by the D_{3d}^6 space group of Al_2O_3. A small change in this mean position on excitation into the ^2E state would explain the lack of mirror symmetry between absorption and emission.

4. LIFETIME MEASUREMENTS

The measurement of the lifetime of the ^2E metastable state of the Cr^{3+} ion in ruby, though straightforward at high temperatures, is made difficult at low temperatures ($T\lesssim150$°K) by the self-absorption of fluorescence. This lengthens the fluorescent decay time of the crystal as a whole over that of an individual Cr^{3+} ion. Varsanyi and co-workers[7] found that the fluorescent decay time, in fact, depended on the size and Cr^{3+} concentration of the sample, varying at 77°K from 4.3±0.3 sec in a dilute dispersed powder to 15 msec in a boule having about 1.6×10^{19} Cr^{3+} ions cm^{-3}.

We have measured the lifetime in both the high- and low-temperature regimes. For measurements at 195,

[31] The sharpest peak in the emission spectrum at 77°K is 376.9 cm^{-1} below the R_1 line and is only $\frac{1}{2}$ cm^{-1} wide. There is a similar peak at the same interval below the R_2 line. A corresponding absorption peak 376.7±0.2 cm^{-1} above the R_1 line is visible at high resolution. Like the rest of the spectrum in this frequency range, it is appreciably weaker in absorption than in emission.

[32] R. E. Dietz, D. G. Thomas, and J. J. Hopfield, Phys. Rev. Letters 8, 391 (1962).

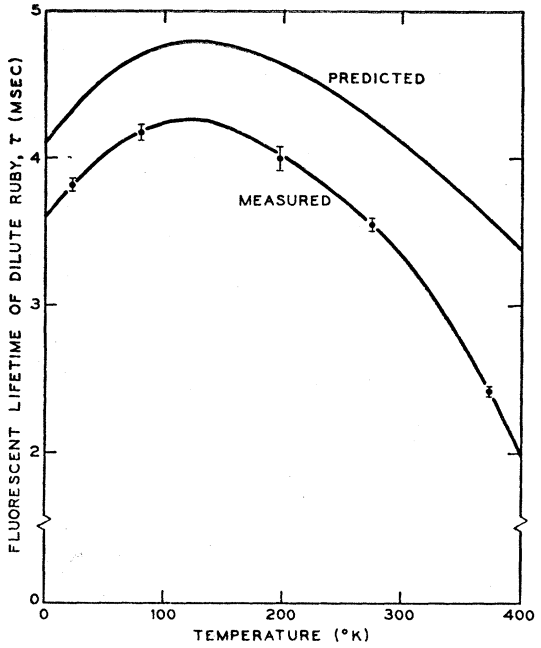

FIG. 6. Fluorescent lifetime of the ^2E levels of ruby, measured in optically thin crystals, as a function of temperature.

273, and 373°K a ruby crystal 1 mm thick by 2 mm diameter containing 1.6×10^{18} Cr^{3+} ions cm^{-3} was used. Under these conditions self-absorption of fluorescence was negligible. The crystal was excited by the green light from a xenon flash tube and the fluorescent decay was recorded on an oscilloscope. The time base was calibrated and the response of the system checked by measuring the exponential decay of a resistor-condenser combination of similar decay time. The fluorescent decay was followed typically for 25 msec and its exponential character checked. About 25 separate measurements were made at each temperature. The results are shown in Fig. 6.

At 20 and 77°K avoidance of lifetime lengthening from self-absorption of fluorescence requires the use of very small and dilute ruby crystals. This requirement also lowers the signal-to-noise ratio, thus necessitating the more elaborate techniques of photon counting. The decaying fluorescence was focused through appropriate red filters onto the input slits of a Jarrell-Ash Model 78–420 spectrometer set on the R_1 line. The photon pulses from a cooled RCA 7102 photomultiplier were fed into an RIDL 400 channel analyzer (Model 34–12*B*).[33] Two nominally undoped sapphire crystals cut from the same boule were studied. They had volumes of $16.5\times4.33\times3.15$ and $8.5\times4.3\times0.36$ mm^3 and contained less than 6×10^{16} Cr^{3+} ions cm^{-3}, as determined from absorption in the green and violet.[8] *R*-line emission could easily be detected, however. Least squares fits of exponentials to the channel counts (after background subtraction) led to lifetimes about 1% smaller for the smaller crystal at 20°K and less than 1% smaller at 77°K. Since the volumes of the crystals differed by a factor of 20, the lifetime of the smaller sample was taken as the true value for isolated Cr^{3+} ions. These results are also shown in Fig. 6.

As seen from Fig. 6 the lifetime in dilute ruby has an interesting temperature dependence. While in many fluorescent solids the lifetime rises monotonically as the temperature is lowered, here it is seen to pass through a maximum. The shortening of the lifetime at low temperatures is due, however, to a simple cause: at lower temperatures a greater proportion of the excited-state population resides in the lower metastable state which happens to have the stronger oscillator strength, as seen from Table I. The decreasing lifetime at temperatures above 100°K is primarily due to the increasing strength of the vibronic satellites of the *R* lines and is discussed in Sec. 6. Our results agree well with those of Tolstoi and Liu Shun-Fu[10] above 77°K. These authors did not go to sufficiently low temperatures to observe the drop in lifetime noted above.

The self-absorption of fluorescence can be utilized to measure the lifetime arising only from the vibronic transitions (plus any totally nonradiative transitions if such exist). This lifetime will be the decay time of the metastable levels under conditions where the *R*-line fluorescence is strongly self-absorbed by the crystal but where the vibronic transitions have no appreciable self-absorption. These conditions are low temperature ($T\lesssim100$°K), relatively high Cr^{3+} concentrations (but low enough to avoid significant chromium ion pairing[20]), and large (but not infinite) crystal size. Mathematically the conditions are $\alpha_R l\gg1$ and $\alpha_V l\ll1$ where α_R and α_V are appropriately averaged absorption coefficients in the *R* lines and in the region of vibronic transitions (at the frequencies of emission), respectively, and l a typical optical path length in the crystal.

In general, for the interior of the crystal, we can write the continuity equation for *R*-line photons as

$$\frac{\partial\rho}{\partial t}+\mathrm{div}\rho\mathbf{v}=-\rho v\alpha_R+nf/\tau. \tag{2}$$

Here ρ is the density of photons, $\mathbf{v}$ their velocity, n the density of excited chromium ions, and α_R the absorption coefficient averaged over the *R* lines. As ruby is anisotropic, α, v, and ρ are appropriate averages over orientation. When a few milliseconds have elapsed after the end of the exciting pulse, the following order-of-magnitude relations will hold:

$$\mathrm{div}\rho\mathbf{v}\sim\frac{\rho v}{l},\quad \frac{\partial n}{\partial t}\sim\frac{-n}{\tau},\quad \frac{\partial\rho}{\partial t}\sim\frac{\rho}{\tau}.$$

Under conditions of strong self-absorption, for which $\alpha_R v\tau\gg\alpha_R l\gg1$, and so long as $f\neq1$ (the case $f=1$ is con-

[33] M. V. Klein and G. W. Barton, Rev. Sci. Instr. **34**, 754 (1963).

sidered below) terms on the left-hand side of (2) are small relative to those on the right and we have

$$\frac{nf}{\tau}\approx\rho v\alpha_R. \tag{3}$$

This equation expresses the fact that a quasisteady state is reached, in which the rate of emission in the R lines at any point is equal to the rate of absorption.

The equation of continuity for chromium ions is

$$\frac{\partial n}{\partial t}=-\frac{n}{\tau}+\rho v\alpha_R$$

Substituting from Eq. (3) we get

$$\partial n/\partial t=-(n/\tau)(1-f)$$

which has the general solution

$$n(x,t)=n(x)e^{-t(1-f)/\tau}.$$

Thus the excited ion density decays exponentially at a uniform rate throughout the crystal, and the emission at all wavelengths must decay at the same rate. The quantity $(1-f)/\tau$ is the rate of emission by all processes except the R lines and the inverse of it is the lifetime for all such processes taken together. For electric-dipole radiation in a uniaxial crystal, in which all decay is radiative

$$f=\frac{\tau}{3}\left(\frac{2\eta_\perp}{\tau_\perp}+\frac{\eta_\parallel}{\tau_\parallel}\right), \tag{4}$$

where $\eta_\perp$ and $\eta_\parallel$ are the radiative efficiencies defined in Sec. 2 and $\tau_\perp$ and $\tau_\parallel$ are the inverse transition rates for emission in the R lines with $E\perp c$ and $E\parallel c$, respectively.

Our analysis is inapplicable when $f=1$ [strictly, when $1-f\lesssim(1/\alpha l)$] as the detailed line shape must then be taken into account. The case $f=1$, though not likely to be encountered in solids, holds for resonance lines in gases and has been considered by Holstein.[34] Under conditions of strong self-absorption the decay is determined by the extreme wings of the line, which are not self-absorbed. For a Gaussian line with peak absorption coefficient α_m, Holstein finds that in a semi-infinite slab of thickness l, the lifetime is lengthened by the factor

$$0.94\alpha_m l[\ln(\alpha_m l/2)]^{1/2}.$$

Under the conditions of our experiment this factor is about 2000 at 77°K, while the actual lifetime is lengthened only by a factor of about 4. Clearly the contribution of the wings to the decay is negligible at 77°K and below. For smaller values of αl it is important and is presumably responsible for the unexpectedly small lifetime lengthening observed at the higher temperatures; unfortunately Holstein's calculation is not applicable as the line is Lorentzian at these temperatures. (Crystalline anisotropy is also a serious complication not considered by Holstein.)

To measure the lengthened lifetime $\tau/(1-f)$ we used an 18.9-cm-long 1.59-cm-diam rod containing 1.8×10^{19} Cr^{3+} cm^{-3}, as measured by absorption in the green through the sides. For the lifetime measurement the rod was opaquely silvered on its sides giving an effective diameter of about 80 cm. Green light from a xenon flash tube excited one end of the rod and the fluorescence from the other end was detected by an RCA 7102 photomultiplier with red filters appropriate for isolating either the R lines or the vibronic satellites. The decaying signal was measured until it fell to about a thousandth of its initial value. The decay was accurately exponential and independent of wavelength after the first 6 msec. Measurements of this lengthened lifetime yielded 15.9±0.3 msec (20°K), 15.4±0.2 msec (77°K), 8.31±0.15 msec (195°K), and 5.32±0.05 msec (273°K). At the two lower temperatures the measured lifetime is that of all decay processes except the R lines. At the higher temperatures the measurements are low since the validity conditions, $\alpha_R l\gg1$ and $\alpha_V l\ll1$, are not adequately met, particularly for the π radiation of the R lines.

5. DETAILED BALANCE

The principle of detailed balance is basic to theories of optical transitions in solids.[35–37] By detailed balance we mean that the probability of a transition from state A to state B is the same as that from state B to state A. Here A and B refer to states of the whole crystal, i.e., combined electronic-vibrational states. When lattice relaxation occurs after a Franck-Condon transition, absorption and emission do not occur between the same pair of vibronic states (though the electronic states may be the same) and detailed balance need not in general hold.[35,38] This relaxation manifests itself as a Stokes shift, and a criterion for the transition $A\leftrightarrow B$ to be the same in absorption and emission is simply the absence of such a shift. The R lines (but not, of course, their vibronic satellites) satisfy this criterion, having a Stokes shift of less than two parts in 10^7 (Sec. 3 and Ref. 30). We would therefore expect the R lines alone, but not necessarily their satellites, to obey detailed balance as expressed in the Einstein relation between absorption and spontaneous emission.[35]

Detailed balance in atomic systems was demonstrated experimentally many years ago for a number of resonance lines in monatomic vapors; in particular for the 2288 and 3261 Å lines of Cd,[15] for the yellow doublet of Na,[16] and for the 2536-Å line of Hg.[17,18] It has also been shown to hold to within 10% for a number of organic

[34] T. Holstein, Phys. Rev. 72, 1212 (1947).

[35] D. E. McCumber, Phys. Rev. 134, A299 (1964); 136, A954 (1964).

[36] W. Van Roosbroeck and W. Shockley, Phys. Rev. 94, 1558 (1954).

[37] F. Stern, in *Solid State Physics*, edited by F. Seitz and D. Turnbull (Academic Press Inc., New York, 1963), Vol. 15, p. 364.

[38] W. B. Fowler and D. L. Dexter, Phys. Rev. 128, 2154 (1962).

compounds in solution,[39] in spite of the large Stokes shifts which occur in these systems. While detailed balance has been used to relate experimental data on absorption and emission in semiconductors such as Si,[13] InSb,[14] and GaAs,[40] in all these cases the presence of nonradiative decay has prevented a precise quantitative proof of detailed balance. The most precise study, that on Si,[13] was for indirect phonon-assisted transitions, where a Stokes shift is necessarily present. That study showed that the *shape* of the emission spectrum, consisting of exciton and free hole-electron pair recombination, was predictable from absorption data and the assumption of thermal equilibrium among the excited states. However, no comparison of the *strength* of the emission with that of absorption was possible. So far as we have been able to determine, there is no evidence in the literature that detailed balance in the sense defined above holds with any precision in solids. Previous analyses of such systems as ruby,[7] and others have shown that it holds to within an order of magnitude. We propose to show in this section that detailed balance holds for the R lines of ruby to well within the experimental accuracy of 5%.

The measurements described in this paper check the principle of detailed balance as applied to an entire line; that is, the transition probabilities are equal in absorption and emission when summed over initial and final spin (strictly, time reversed) states. This principle is more correctly called the principle of semidetailed balance, and has been shown[41] to be a consequence of time reversal and space-inversion symmetry. The latter symmetry does not hold in ruby, as the Cr^{3+} ion is not at a center of symmetry (the R lines depend for their strength on this fact). However, it is known (compare Refs. 2 and 7) that in dilute ruby the *relative* intensities of the Zeeman components of the R lines are the same in absorption and emission. It follows from this fact that the present results show that *strict* detailed balance holds for each individual Zeeman component of the R lines. Strict detailed balance is a consequence of the first Born approximation; that is, the replacement of the transition operator by the potential.[42] This replacement is equivalent to neglecting terms in the interaction nonlinear in the potential.[43] In this approximation strict detailed balance applies independently of space-inversion invariance.[35]

The problem in comparing transition probabilities in absorption and emission is not only that absolute photometric measurements are extremely difficult to make but that the number of ions in the excited state during fluorescence cannot in practice be determined accurately. We therefore concentrate on the fluorescent lifetime, which depends on the integrated spontaneous emission and can be measured with considerable accuracy. However, the lifetime is not determined solely by emission in the R lines. Other processes—photon emission with the simultaneous emission of a phonon, and perhaps nonradiative decay—contribute quite substantially. These processes can be distinguished by the fact that they cannot occur in absorption at low temperatures; thus in a sufficiently thick and concentrated crystal, in which the R lines are completely self-absorbed, the lifetime will be determined entirely by them. Let the lifetime observed under these conditions be τ_V, and the emission probability in the R lines τ_R^{-1}. Then the lifetime τ in a very thin crystal, where self-absorption in the R lines can be neglected, is given by

$$\tau^{-1}=\tau_R^{-1}+\tau_V^{-1}. \tag{5}$$

Thus the measurements of τ and $\tau_V[=\tau/(1-f)]$, described in Sec. 4, suffice to determine τ_R. It is necessary to average not only over both polarizations but also over the two R lines, which must be weighted according to the population of their initial states (which are in thermal equilibrium and have equal statistical weights). We find

$$\tau_R^{-1}=[1+\exp(\Lambda/kT)]^{-1}[\tau_{R_1}^{-1}\exp(\Lambda/kT)+\tau_{R_2}^{-1}], \tag{6}$$

where Λ is the splitting of the ^2E level. Equation (6) assumes a temperature low enough ($\lesssim$150°K) that the $^2T_1$ levels are unpopulated. The transition probability for absorption can be formally expressed as an emission lifetime through the Ladenberg formula.[44] For electric-dipole radiation in a uniaxial crystal the Ladenberg formula may be written

$$\tau_{R_1}^{-1}=16\pi\mu_r^2\nu^2 c\int_{R_1}(\tfrac{2}{3}\sigma_\perp+\tfrac{1}{3}\sigma_{11})d\nu \tag{7}$$

and similarly for τ_{R_2}. Here ν is in cm^{-1}; $\sigma_\perp$ and σ_{11} are the absorption cross sections from Sec. 3; the refractive index μ_r is that of the bulk crystal without local field corrections (its small anisotropy is neglected); we have summed over polarization, and the ratio of lower to upper state degeneracy ($=2$) has been included.[45] The data are summarized in Table III. Comparison of the last two columns of Table III shows that at 77° and 20°K detailed balance holds to well within the experimental accuracy of ±5%. A similar comparison at higher temperatures is not possible as the necessary conditions for

[39] S. J. Strickler and R. A. Berg, J. Chem. Phys. **37**, 814 (1962). (We are grateful to Professor D. L. Dexter for drawing our attention to this paper.)

[40] K. Konnerth and C. Lanza, Appl. Phys. Letters **4**, 120 (1964); J. C. Sarace, R. H. Kaiser, J. M. Whelan, and R. C. C. Leite, Phys. Rev. **137**, A623 (1965).

[41] F. Coester, Phys. Rev. **84**, 1259 (1951).

[42] J. M. Jauch and F. Rohrlich, in *Theory of Photons and Electrons* (Addison-Wesley Publishing Company, Cambridge, Massachusetts, 1955), pp. 142, 319.

[43] W. Heitler, in *Quantum Theory of Radiation* (Oxford University Press, New York, 1954), 3rd ed., p. 162.

[44] R. Ladenberg, Z. Physik **4**, 451 (1921).

[45] This factor cancels the effect of averaging over the two components of the R line, as was done in Table II in order to make the results at low and high temperatures directly comparable. The same result would, of course, be obtained by adding together the contribution of each component to the transition probability. [See Eq. (10).]

TABLE III. Comparison of the emission and absorption probabilities in the R lines to check the principle of detailed balance. The transition probability τ_R^{-1} is calculated from the emission data by Eq. (5) and from the absorption data by Eqs. (6) and (7).

	Emission			Absorption
T (°K)	τ^{-1} (sec^{-1})	τ_V^{-1} (sec^{-1})	τ_R^{-1} (sec^{-1})	τ_R^{-1} (sec^{-1})
77	239±3	65±1	174±3	173±7
20	262±3	63±1	199±3	189±10

the measurement of τ_V can no longer be met. A substantial amount of π radiation in the R lines can escape from the crystal without being self-absorbed.

The demonstration of detailed balance in the R lines confirms the adequacy of the first Born approximation in treating light emission and absorption. This is, of course, hardly surprising: deviations from the first Born approximation manifest themselves as nonlinear effects which are not observed at the low light intensities used in the present experiments.

6. TEMPERATURE DEPENDENCE OF THE FLUORESCENT LIFETIME

Although we were unable to determine τ_R at temperatures above 100°K directly from emission measurements, we can still compare the actual fluorescent lifetime τ with the radiative lifetime calculated from the observed absorption in the R lines and the radiative efficiencies. This calculation is purely phenomenological and does not depend on any particular model, but does ignore nonradiative decay. The rate of emission in k polarization in the sharp line connecting the ith excited state with a component of the ground state is[35]

$$\tau_{ik}^{-1}=\lambda_i^{-2}\exp[\hbar(\mu-\omega_i)/kT]\int_{4\pi}d\Omega\int_i\sigma_k(\omega)\frac{d\omega}{2\pi}, \quad (8)$$

where σ_k is the absorption cross section in k polarization, which we integrate over the ith line, $\lambda_i=2\pi c/\omega_i\mu_r$ is the wavelength of the line in the medium, and $\hbar\mu$ is the chemical potential discussed below. If a fraction η_{ik} of the total number of k-polarized photons emitted from state i is emitted in the sharp line, the total rate of emission from this state is $\eta_{ik}^{-1}\tau_{ik}^{-1}$. Summing over i and k, and integrating over solid angle Ω for electric-dipole radiation in a uniaxial crystal we find for the lifetime due to all radiative processes:

$$\tau^{-1}=4\pi e^{\hbar\mu/kT}\sum_i\lambda_i^{-2}e^{-\hbar\omega_i/kT}\times\int_i[\tfrac{4}{3}(\sigma_1/\eta_1)+\tfrac{2}{3}(\sigma_{11}/\eta_{11})]d\omega/2\pi. \quad (9)$$

As defined in Ref. 35, $\hbar\mu$ is the difference between the chemical potential of the manifold of excited states (assumed to be in thermal equilibrium with each other)[46] and that of the ground state. Thus $\hbar\mu=kT\ln(Z_g/Z_{ex})$ where Z_g and Z_{ex} are partition functions for the ground-state and the excited-state manifolds, respectively. If the phonon states are the same for all the excited states and the ground state, their contributions to Z_g and Z_{ex} cancel, and we have

$$e^{-\hbar\mu/kT}=Z_{ex}/Z_g=\tfrac{1}{2}\sum_{i=1}^{5}e^{-\hbar\omega_i/kT}. \quad (10)$$

The ground state is quadruply degenerate (we neglect its small splitting) while the five substates of ^2E and $^2T_1$ are doubly degenerate.

We cannot use Eq. (9) as it stands, however, as we cannot distinguish experimentally between emission from the $^2T_1$ levels and vibronic satellites of the R lines (phonon assisted emission from the ^2E levels). In fact, the measured "vibronic satellites" from which we derived the radiative efficiency, include both the no-phonon $^2T_1\rightarrow{}^4A_2$ lines and their phonon-assisted emission. This part of the sum in Eq. (9) is therefore included in the R_1 and R_2 terms, and we have finally

$$\tau^{-1}=16\pi c\mu_r^2\left\{\sum_{i=1,2}\nu_i^2e^{-\hbar\omega_i/kT}\times\int_i[\tfrac{2}{3}(\sigma_1/\eta_1)+\tfrac{1}{3}(\sigma_{11}/\eta_{11})]d\nu\Big/\sum_{i=1}^{5}e^{-\hbar\omega_i/kT}\right\}, \quad (11)$$

where $\eta_\perp$ and η_{11} are the measured radiative efficiencies[47] and $\nu=(\mu_r\lambda)^{-1}$ is in cm^{-1}. It is convenient when using Eq. (11) to cancel a factor $e^{-\hbar\omega_1/kT}$ top and bottom and measure all ω from ω_1, the frequency of the R_1 line (note that as $T\rightarrow0$, $\mu\rightarrow\omega_1$). When this is done, and the $^2T_1$ terms ($i=3, 4, 5$) dropped from the denominator because of the low temperature, Eq. (11) is exactly analogous to Eqs. (6) and (7) combined.

The assumption made in the calculation of μ, that the phonon states are independent of the electronic state, is not justified when the vibronic satellites are not

[46] That the ^2E levels are in equilibrium with each other is shown by the fact that the intensity ratio of the R_1 to the R_2 line in emission follows the Boltzmann Law $I_2/I_1=\exp(-h\nu/kT)$ with $\nu=29.2$ cm^{-1} [see P. Pringsheim in *Fluorescence and Phosphorescence* (Interscience Publishers, 1949), p. 641]. That the $^2T_1$ levels are in thermal equilibrium with the ^2E levels at room temperature has been implicity demonstrated by E. Bukke and Z. L. Morgenshtern, Opt. i. Spektroskopiya 14, 687 (1963) [English transl.: Opt. Spectry. (U.S.S.R.) 14, 362 (1963)] who showed that the anti-Stokes emission is the same whether excited by absorption in the green band or in the R lines themselves. It is shown in Sec. 7 that much of the anti-Stokes emission arises from the $^2T_1$ levels. We have measured the intensity of emission from each of the $^2T_1$ levels as a function of temperature and find that in both cases it follows the Boltzmann law with ν the separation of the level from the ^2E levels.

[47] The values of $\eta_\perp$ and η_{11} put into this equation are the measured values at the temperature concerned. The fact that the two R lines may have different η_{11} does not affect the calculation, as the relative contribution of each line in Eq. (11) is the same to the lifetime as it is to η. This does not apply to the calculation of Sec. 7.

equivalent in absorption and emission (see Sec. 3). However, we expect the effect of this difference to be small because of the weakness of the satellites relative to the $^4A_2 \rightarrow {}^2T_1$ lines (see Fig. 5).

The values of τ^{-1} calculated from Eq. (11) are given in the sixth column of Table II and are plotted in Fig. 6. In the calculation of μ we have used the values of $\nu_i (i=1, 2, 3, 4, 5)$ given in Fig. 1.[3] The seventh column gives the observed values of τ^{-1}. The discrepancy between the observed and calculated values of τ^{-1} is given in the last column. The discrepancy, with its rapid rise at temperatures above 200°K, is probably due to nonradiative decay. However, the small and relatively constant discrepancy at low temperatures could possibly represent a long tail to the vibronic band, too weak to be detectable in our experiments (it would have to extend over at least 5000 cm^{-1} to explain the discrepancy).

7. TEMPERATURE DEPENDENCE OF RADIATIVE EFFICIENCY

In the previous section we used the observed radiative efficiency and integrated absorption cross section at any given temperature to calculate the radiative lifetime at that temperature. We now use a simple model to predict what the temperature dependence of the radiative efficiency should be, using the emission and absorption data at 77°K. The model is that of an impurity center in which the electronic states are weakly coupled to the lattice by one-phonon interactions; that is, the center exchanges energy with the lattice in single quanta only.

It is convenient and sufficiently accurate to ignore the splitting of the ^2E level and to lump the R_1 and R_2 lines together at a frequency w_R and, to measure ω from ω_R. We may write for the radiative efficiency in a given polarization

$$\eta(T)=R(T)/[R(T)+S(T)+U(T)],$$

where $R(T)$ is the integrated emission in the R lines at the temperature T, $S(T)$ the integrated emission at frequencies below the R lines ($\omega<0$, Stokes emission) and $U(T)$ the integrated emission at frequencies above the R lines ($\omega>0$, anti-Stokes emission). The probability $A_k(\omega,T)$ of spontaneous emission in k polarization (per unit frequency interval and solid angle) can be expressed in terms of the absorption cross section $\sigma_k(\omega,T)$ by the Einstein relation[48] written in the form[35]

$$A_k(\omega,T)=\lambda^{-2}\sigma_k(\omega,T)e^{\hbar(\mu-\omega)/kT}, \qquad (12)$$

where $\lambda=2\pi c\mu_r^{-1}(\omega+\omega_R)^{-1}$, and μ is defined in Sec. 6. For weak electron-phonon coupling[49]

$$\sigma_k(\omega,T)=(4\pi^2/\hbar\lambda)|P_k|^2 e^{-\gamma(T)} \times[\delta(\omega)+(\rho_k(\omega)/\omega^2)\{n(\omega,T)+\theta(\omega)\} +\text{multiphonon terms}]. \qquad (13)$$

Here P_k is the electric-dipole matrix element for the $^4A_2 \rightarrow {}^2E$ transition, assumed to be independent of phonon coordinates[50] though not necessarily of temperature (see Sec. 3) and to include local-field corrections. In the one-phonon term $|\omega|$ is the phonon frequency, $n(\omega,T)=[e^{\hbar|\omega|/kT}-1]^{-1}$ is the phonon occupation number, $\theta(\omega)$ is the step function 1 for $\omega>0$ (phonon emission) and 0 for $\omega<0$ (phonon absorption), $\rho_k(\omega)$ is an effective density of phonon states (true density of states multiplied by a frequency- and polarization-dependent coupling parameter). The factor $e^{-\gamma(T)}$ is the normalizing factor $e^{-\gamma_G}$ defined in Ref. 49. The δ function represents the R lines. The integrated emission in the R lines $R(T)=e^{\Gamma}p_k(T)R(0)$, where $\Gamma=\hbar\mu/kT+\gamma(0)-\gamma(T)$, and $p_k(T)=|P_k(T)|^2/|P_k(0)|^2$. The Stokes emission is

$$S_k(T)=\int_{-\omega_R}^{0} A_k(\omega,T)d\omega = e^{\Gamma}p_k(T)\int_{-\omega_R}^{0} A_k(\omega,0)[n(\omega,T)+1]d\omega \qquad (14)$$

when multiphonon processes are neglected. $A_k(\omega,0)$ is the emission at 0°K (77°K, where anti-Stokes emission is still negligible, is sufficiently near zero for our purposes). Emission in the R lines themselves (i.e., emission within a few cm^{-1} of ω_R) is excluded from $A_k(\omega,0)$.

From Eq. (12) we have for the anti-Stokes emission

$$U_k(T)=\int_0^{\infty} A_k(\omega,T)d\omega = e^{\hbar\mu/kT}\int_0^{\infty}\lambda^{-2}\sigma_k(\omega,T)e^{-\hbar\omega/kT}d\omega. \qquad (15)$$

If $\rho(\omega)=\rho(-\omega)$ as might be expected for such a weakly coupled system, we would have from Eq. (13) (for $\omega>0$)

$$\sigma_k(\omega,T)=\sigma_k(-\omega,T)\frac{\lambda(-\omega)}{\lambda(\omega)}\frac{n(\omega,T)+1}{n(\omega,T)} =A_k(-\omega,T)e^{-\hbar\mu/kT}\frac{[\lambda(-\omega)]^3}{\lambda(\omega)}. \qquad (16)$$

The data shown in Fig. 5 demonstrate that Eq. (16) does not hold at 77°K, where $\mu=0$. This conclusion is confirmed for higher temperatures by the detailed shape of the anti-Stokes emission, as follows. If Eq. (16) holds, we have

$$A_k(\omega,T)=A_k(-\omega,T)e^{-\hbar\omega/kT}\left[\frac{\lambda(-\omega)}{\lambda(\omega)}\right]^3. \qquad (17)$$

[48] A. Einstein, Physik. Z. **18**, 121 (1917).
[49] D. E. McCumber, Phys. Rev. **135**, A1676 (1964).
[50] For the case where this assumption is dropped, and for the more precise definition of $\rho(\omega)$, see Ref. 49. For a discussion of the physical significance of $\rho(\omega)$, see F. Imbusch, W. Yen, A. L. Schawlow, D. E. McCumber, and M. D. Sturge, Phys. Rev. **133**, A1029 (1964).

Figure 7 shows the spontaneous emission as a function of frequency at 373°K, expressed as a cross section; the dotted line represents the emission for $\omega>0$ calculated from the emission for $\omega<0$ and Eq. (17). For small Ω the emission is less than calculated; i.e., $\rho(\omega)<\rho(-\omega)$ $(\omega>0)$. For larger ω the $^2T_1$ levels dominate the emission which is therefore much greater than calculated. Clearly we cannot use the low-temperature emission data to calculate the anti-Stokes term, but must use the absorption data and Eq. (15).

For that part of $\sigma_k(\omega,T)$ which is due to absorption into the ^2E levels with phonon emission, we can use Eq. (13) and write

$$\sigma_k{}^E(\omega,T)=e^{\gamma(0)-\gamma(T)}p_k(T)\sigma_k{}^E(\omega,0)[n(\omega,T)+1]$$

so that this part of $U_k(T)$ is given by

$$U_k{}^E(T)=e^{\Gamma}p_k(T)\int_0^\infty \lambda^{-2}\sigma_k{}^E(\omega,0)n(\omega,T)d\omega. \quad (18)$$

It is a reasonable approximation to suppose that the matrix element for the $^4A_2\rightarrow{}^2T_1$ transition has the same temperature dependence $p_k(T)$ as that of the $^4A_2\rightarrow{}^2E$ transition since both transitions derive their strengths primarily from the $^4A_2\rightarrow{}^4T_2$ band.[1] It is convenient to treat the vibronic satellites of the $^4A_2\rightarrow{}^2T_1$ lines as if they had the same strengths relative to the no-phonon lines as those of the R lines. This assumption is analogous to the neglect of multiphonon effects, and the error is partly canceled on integrating over frequency. Then we may write for absorption into the $^2T_1$ level $\sigma_k{}^T(\omega,T)=e^{\Gamma}p_k(T)\sigma_k(\omega,0)$ (where we have neglected any change of the $^2T_1-{}^2E$ separation with temperature). We now note that for $T\lesssim 400$°K and $\omega\gtrsim 500$ cm^{-1} (the lowest $^2T_1$ level) $n(\omega,T)\approx e^{-\hbar\omega/kT}$, so Eq. (18) applies with sufficient accuracy for emission from the $^2T_1$ levels and we can add the terms in σ^T and σ^E to find[51]

$$U_k(T)=e^{\Gamma}p_k(T)\int_0^\infty \lambda^{-2}\sigma_k(\omega,0)n(\omega,T)d\omega. \quad (19)$$

Substituting for $R(T)$, $S(T)$, and $U(T)$ in Eq. (11), we find

$$\eta_k{}^{-1}=1+R_k{}^{-1}(0)\int_{-\omega R}^{0} A_k(\omega,0)[n(\omega,T)+1]$$

$$+\lambda_R{}^2\left[\int_R \sigma_k d\omega\right]^{-1}\int_0^\infty \lambda^{-2}\sigma_k(\omega,0)n(\omega,T)d\omega, \quad (20)$$

where the terms in the right-hand side are normalized to the R lines in the same way as the experimental data. Note that the factor e^{Γ} has canceled out, so that the temperature dependence of γ is of no consequence. We are therefore unable to determine from the radiative efficiency whether or not the satellites are induced by the odd-parity component of the crystal vibrations.

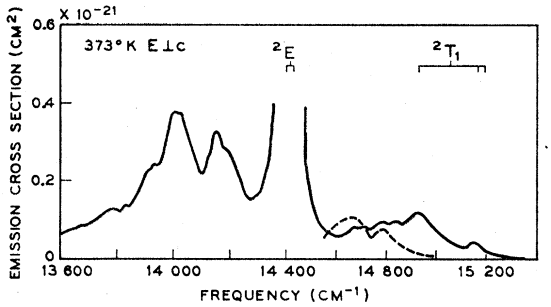

FIG. 7. Emission spectrum of ruby at 373°K, converted to emission cross section as in Fig. 5. The dotted curve shows the emission for $\omega<0$ calculated from the emission for $\omega<0$ by Eq. (17).

We have calculated $S(T)$ and $U(T)$ for both polarizations from the observed emission and absorption at 77°K and used Eq. (20) to calculate the curves shown in Fig. 2. Both curves may be somewhat high due to the neglect of multiphonon effects, and the imprecise treatment of phonon-assisted transitions from the $^2T_1$ levels.[51] For π polarization, two sources of error, in addition to the neglect of multiphonon effects, are important. These are the neglect of the difference between $\eta_{11}(R_1)$ and $\eta_{11}(R_2)$ (see Ref. 47) and the presence of imperfect polarization in the excitation spectrum, which can lead to too large an anti-Stokes term calculated from Eq. (14). These errors could make the calculated η_{11} too low by up to 0.04 at 373°K.

In view of the approximations made, the fit of the calculated curves to experiment demonstrated in Fig. 2 is good, and shows that our model for the electron-phonon interaction is reasonably adequate.

8. LASER IMPLICATIONS

The present work has a number of implications concerning ruby lasers. The proof of detailed balance and the demonstration of the absence of a Stokes shift in the R lines confirms the validity of the often-used laser model in ruby[52] where the absorption cross section is used for the stimulated emission cross section. The demonstration that the integrated strength of the R lines is approximately independent of temperature up to nearly room temperature justifies the procedure[52] of taking the peak absorption cross section inversely proportional to the linewidth[53] for $300°\text{K}\gtrsim T\gtrsim 100°\text{K}$.

[51] Note that in Eq. (19) we have neglected to distinguish between anti-Stokes emission from the ^2E levels and Stokes emission from the $^2T_1$ levels in the same frequency range; this introduces an error comparable with that due to neglect of multiphonon effects.

[52] D. F. Nelson and J. P. Remeika, J. Appl. Phys. 35, 522 (1964).

[53] In principle one should be careful to allow for the change of line shape from Lorentzian to Gaussian as the temperature is lowered. In practice, however, this effect is small, as the increase in peak height (relative to area divided by width) due to the change from Lorentzian to Gaussian is largely compensated by the resolution of the isotopic structure at low temperatures, and the small decrease in integrated absorption noted in Table II.

In one study of the ruby-laser threshold population distribution at 77°K[54] some of the data could not be accounted for by a theoretical model. From the present work it appears that a contributing cause was an inadequate knowledge of the radiative efficiencies and the spontaneous emission lifetime. With the results of this present study a reevaluation of that threshold study might be useful.

It is interesting to inquire whether laser oscillation could be obtained using the vibronic transitions (Stokes radiation) in ruby in the manner recently reported in $MgF_2:Ni^{2+}$ crystals.[55] For temperatures of 77°K or lower there is negligible absorption at the emission wavelengths. Though attainment of stimulated emission at these wavelengths is thus guaranteed for even low excitation levels, the gain coefficient attainable is low because of the very weak oscillator strength of the vibronic transitions. The peak emission cross section in the vibronic transitions from Fig. 5 of 3.0×10^{-22} cm^{-2} gives a gain coefficient[56] of 0.01 cm^{-1} for an excitation density of the metastable levels of 1.6×10^{19} cm^{-3}, corresponding to a 50% excitation for the Cr^{3+} ions in 0.1 wt% Cr_2O_3 ruby. A gain of 10% per pass results for a 10-cm-long rod. If absorption of fluorescence by the metastable-level population is as low as recently indicated[57] and if scattering and reflectance losses can be held to a few percent per pass, laser oscillation should be possible. A resonator should be used which is very lossy at the wavelength of the R_1 line to prevent its oscillation if it too becomes inverted. Incorporation of a dispersive element, such as a prism,[58] in the resonator could accomplish this.

Gires and Mayer[59] found an anomalously low threshold for a ruby laser operated at room temperature. To explain this result, they proposed a model which requires the existence of vibrational modes which have a higher frequency when the chromium ion is in the ^2E state than when it is in the $^4A_2$ ground state. Our observations of the vibronic transitions near the R lines (see Fig. 5) give no evidence for such states, though the presence of the nearby $^2T_1$ levels makes observation of the higher lying vibronic states in absorption quite difficult. It should be pointed out that the existence of these $^2T_1$ levels, which act as a useless storage location for excited atoms for temperatures above 200°K,[52] raises laser threshold. The anomalous threshold results of Ref. 59 could be accounted for by a greater density of vibrational states associated with the electronic ground state compared with that associated with the ^2E states. This would lead to a greater strength of the vibronic transitions near the R lines in emission than in absorption as observed (Fig. 5). However, the similarity *in shape* of the Stokes transitions in emission and absorption, found here, argues for a similar density of vibrational states in the two cases (see Sec. 3) and hence that the difference in strength arises from the different character of the vibronic state involved in the emission and absorption processes. Recently, Aagard and Dufault[57] have repeated the Gires-Mayer experiments, obtaining results consistent with the conventional threshold theory in which differences between absorption and emission are neglected.

ACKNOWLEDGMENTS

We are grateful to J. D. Struthers for making the neutron activation measurements; to Miss D. M. Dodd for the measurements of chromium concentration by optical absorption; to F. R. Merritt for making the spin resonance measurements; to G. E. Devlin for making the photon-counting measurements; to K. F. Rodgers, Jr. and K. A. Ingersoll for technical assistance; and to M. Lax, D. A. Kleinman, and D. E. McCumber for many helpful discussions.

[54] D. F. Nelson and D. E. McCumber, in *Quantum Electronics, Proceedings of the Third International Conference*, edited by P. Grivet and N. Bloembergen (Columbia University Press, New York, 1964), p. 1037.

[55] L. F. Johnson, R. E. Dietz, and H. J. Guggenheim, Phys. Rev. Letters **11**, 318 (1963).

[56] Because of the absorption-emission discrepancy found in these vibronic transitions, the absorption cross section cannot be used for this calculation. Also, since a statistical weight ratio of final to initial states of two has been included in Fig. 4, the gain coefficient is twice the emission cross section times the excited-state population density [R. J. Collins and D. F. Nelson, in *Proceedings of the Conference on Optical Instruments, 1961* (Chapman and Hall Ltd., London, 1962), p. 441].

[57] R. L. Aagard and R. H. Dufault, Appl. Phys. Letters **4**, 102 (1964).

[58] A. D. White, Appl. Opt. **3**, 431 (1964).

[59] F. Gires and G. Mayer, in *Quantum Electronics, Proceedings of the Third International Conference*, edited by P. Grivet and N. Bloembergen (Columbia University Press, New York, 1964), p. 841.